JOURNAL OF VIROLOGY, Nov. 1990, p. 5306–5316
0022-538X/90/115306-11$02.00/0

Vol. 64, No. 11

Transport and Assembly of *gag* Proteins into Moloney Murine Leukemia Virus

MARK HANSEN, LAURA JELINEK, SAM WHITING, AND ERIC BARKLIS*

Vollum Institute for Advanced Biomedical Research and Department of Microbiology and Immunology, Oregon Health Sciences University, Portland, Oregon 97201

Received 23 April 1990/Accepted 27 July 1990

We have studied the process of Moloney murine leukemia virus (M-MuLV) assembly by characterization of core (*gag*) protein mutants and analysis of wild-type (wt) *gag* proteins produced by cells in the presence of the ionophore monensin. Our genetic studies involved examination of linker insertion mutants of a Gag-β-galactosidase (Gag-β-gal) fusion protein, GBG2051, which is incorporated into virus particles when expressed in the presence of wt viral proteins. Analysis indicated that the amino-terminal two-thirds of the *gag* matrix domain is essential for targeting of proteins to the plasma membrane; mutant proteins localized to the cytoplasm or were trapped on intracellular membranes. Mutations through most of the coding region of the *gag* capsid domain generated proteins which were released from cells in membrane vesicles but not in virions. In contrast, linker insertions into p12^{gag} or carboxy-terminal portions of the matrix or capsid coding regions did not affect assembly of fusion proteins into virus particles. Monensin, which blocks vesicular transport, inhibited *gag* protein intracellular transport and release from cells. Our results suggest that a significant proportion of M-MuLV myristylated *gag* proteins travel via vesicles to the cell surface. Specific matrix protein polypeptide regions and myristic acid modification are both necessary for appropriate *gag* protein transport, while capsid protein interactions appear to mediate the final phase of virion formation.

The process of retrovirus assembly requires that several viral constitutents must localize to the plasma membrane of an infected cell and assemble into a budding virus particle. Incorporated into virions are the viral genomic RNAs; core (*gag*) and envelope (*env*) proteins; and viral enzymatic functions, including *pol* gene products such as reverse transcriptase. Central to this process is the retroviral *gag* polyprotein. With Moloney murine leukemia virus (M-MuLV), the *gag* polyprotein is synthesized as a myristylated precursor, Pr65^{gag}, which is cleaved during assembly to form the mature M-MuLV *gag* proteins p15 (matrix, MA), p12, p30 (capsid, CA), and p10 (nucleocapsid, NC) (2, 4, 15, 29, 35, 42). Evidence suggests that synthesis of the M-MuLV *gag* proteins is necessary and sufficient for assembly of (noninfectious) virus particles (14, 23, 33, 40) and that M-MuLV enzymes initially are incorporated into virions as a *gag-pol* fusion protein, Pr180$^{gag\text{-}pol}$ (41).

One clear requirement for virus assembly is a myristic acid addition at the amino-terminal glycine of the matrix domain of Pr65^{gag} (15, 31). This modification appears to be necessary for a membrane association event which is a prerequisite for virion formation (31). While myristylation is essential for *gag* protein membrane association, the mechanism by which myristylated Pr65^{gag} travels to the plasma membrane is unclear. It is possible that myristylated Pr65^{gag} transits freely through the cytoplasm to assembly sites at the inner face of the plasma membrane. Alternatively, *gag* and *gag-pol* proteins may associate with intracellular membranes shortly after synthesis and travel to the cell surface via vesicular transport (17). Also unresolved are details concerning *gag* protein assembly resulting in the formation of a budded virus particle.

To investigate the process of M-MuLV virion formation, we previously expressed Gag-β-galactosidase (Gag-β-gal, GBG) fusion proteins in Psi2 cells (17), which express wild-type (wt) M-MuLV proteins (26). During these studies, we identified a construct (GBG2051; Fig. 1B) encoding a fusion protein which was incorporated efficiently into virus particles and also released from cells in a low-density nonviral form. While GBG2051, containing intact *gag* matrix, p12, and capsid coding regions, was assembled into virions, fusion proteins with deletions in the capsid or capsid plus p12 region were released from cells only in the nonviral form. Also excluded from virions were Gag-β-gal fusion proteins containing only myristylated fragments of the *gag* matrix domain. These proteins were trapped at intracellular membranes, reminiscent of the intracellular trapping of mutant integral plasma membrane proteins (12, 22, 32).

With the goal of clarifying the processes of M-MuLV *gag* protein transport and assembly, we have extended our analysis of Gag and Gag-β-gal fusion proteins. In particular, we have characterized a myristyl-minus version of the GBG2051 fusion protein, as well as 11 linker insertion mutants of the GBG2051 fusion protein. We have also studied the effect of monensin, an inhibitor of vesicular traffic (5, 16, 19, 34), on the transport and release of Gag, Gag-Pol, and Gag-β-gal proteins from cells. Our results indicate that interactions involving the amino-terminal two-thirds of the *gag* capsid domain are essential for incorporation of proteins into virus particles, whereas mutations in p12 and the carboxy-terminal portions of the matrix and capsid domains do not impair assembly into virions. As expected, mutations in the amino-terminal regions of the matrix protein affect the intracellular transport of fusion proteins and may result in the loss of membrane association or in trapping of proteins at intracellular membranes. These results, in conjunction with our observation that monensin inhibits transport and release of Gag, Gag-Pol, and Gag-β-gal proteins, suggest that a large proportion of myristylated Pr65^{gag} travels via vesicular transport to assembly sites at the plasma membrane.

* Corresponding author.

MATERIALS AND METHODS

Cell culture. Psi2 cells (26) and PA317 cells (27) were grown as described previously (3). Psi2 cells populations expressing BAG (7) or GBG constructs were generated by transfection of PA317 cells, infection of Psi2 cells with the PA317 supernatant collected 24 h after transfection, and selection of Psi2 cells with G418 as described previously (17).

Recombinant plasmids. Freak plasmids are derived from pFreak, a plasmid generated by circularizing the neomycin resistance gene-containing *Xho*I cassette of MP10 (3). In pFreak derivatives, the original *Eco*RI site of pFreak was altered to make the following sequences: *Bam*HI-Freak, GAATTCGGATCCGAATTC; *Cla*I-Freak, GAATTCATCG ATGAATTC; *Eco*RV-Freak, GAATTCGATATCGAATTC (Fig. 1). All recombinant retroviral constructs were derived from the β-gal expression vector BAG (7), which was generously provided by Connie Cepko. Construction and sequencing methods followed standard protocols (25). The construct GBG2051, described by Jones et al. (17), encodes an M-MuLV Gag-β-gal fusion protein which includes the M-MuLV *gag* matrix, p12, and capsid domains fused to the ninth residue of β-gal. When expressed in Psi2 cells, this protein is efficiently incorporated into virions (17). GBG myr$^-$ is identical to GBG2051 except for a mutation at the second *gag* codon which prevents myristylation. This mutation was present in a construct kindly provided by Alan Rein (31) and was inserted into the GBG2051 backbone.

All GBG 12in constructs are identical to the GBG2051 parent construct except for 12-bp linker insertions in their gag coding regions. Linker insertions were created as described in the legend to Fig. 1. Briefly, *Eco*RI-minus, ampicillin resistance-conferring target plasmids containing the 5′ portion of the M-MuLV proviral genome up to viral nucleotide (nt) 2051 (34) were randomly linearized and ligated to compatible ends of plasmids *Eco*RV-Freak, *Cla*I-Freak, and *Bam*HI-Freak. Recombinants were selected in bacteria with ampicillin plus kanamycin. After sequencing of insertion sites, 12-bp insertions in target plasmids were generated by deletion of the large Freak-derived *Eco*RI fragment from recombinants. Target plasmids with linker insertions were used to replace wt GBG2051 *gag* coding regions, yielding GBG 12in plasmids. Eleven linker insertion mutation constructs (GBG 12in 676, 747, 919, 1074, 1084, 1436, 1560, 1672, 1752, 1862, and 1908; Fig. 1B) were produced in this fashion. Sequences in mutated regions are shown in Fig. 1C.

Analytical procedures. Enzyme assays, cell fractionation, virus pelleting, sucrose density gradients, immunoblotting, and immunofluorescence protocols were performed as described previously (10, 13, 17, 24 28).

Antibodies and Golgi localization. Mouse anti-β-gal antibody was from Promega Biotec and was used at a 1:3,000 dilution for immunofluorescence studies. A goat anti-feline leukemia virus gp71 antibody, at a 1:1,500 dilution, was used for immunodetection of M-MuLV envelope proteins. Tissue culture supernatants of rat hybridoma cells R187 and R548 (8) were used at 1:2 dilutions for immunoblotting and immunofluorescence detection of M-MuLV p30^{gag} and p12^{gag} proteins, respectively. These cells were the kind gift of Bruce Chesebro. For immunoblotting studies, alkaline phosphatase-conjugated anti-immunoglobulin G (IgG) (Promega Biotec or Boehringer Mannheim) was used at a 1:7,500 dilution. For immunofluorescence, rhodamine-conjugated goat anti-mouse IgG antibody (TAGO) was used at a 1:100 dilution. Golgi complex localization by fluorescein isothiocyanate (FITC)-conjugated wheat germ agglutinin (U.S. Biochemicals) was done by the protocol of Rose and Bergmann (32), but without preincubation with unconjugated wheat germ agglutinin.

Monensin treatment. Monensin was from Sigma Chemical Co. and was stored as a 10 mM stock in ethanol at −20°C. For immunofluorescence studies, 10 or 25 μM monensin was added to cells on cover slips for 4 h prior to fixation. For enzyme or protein analysis, confluent or nearly confluent 10-cm plates of cells were treated for 1 or 3 h at 37°C with 10 ml of Dulbecco modified Eagle medium plus penicillin, streptomycin, and 10% heat-treated calf serum (DMEM/calf) plus 10 or 25 μM monensin. Following this treatment, cells were washed with DMEM/calf and reincubated for 5 or 6 h at 37°C with DMEM/calf plus monensin, after which cells and medium supernatants were collected for analysis.

RESULTS

Assembly of Gag-β-gal proteins into virus particles. In our previous experiments (17), we established a system for studying the assembly of Gag-β-gal fusion proteins into M-MuLV virions. In those studies, fusion proteins were expressed in Psi2 cells, which produce wt M-MuLV proteins, and the ability of fusion proteins to become incorporated into virus particles was analyzed. Our negative control construct, BAG, expressed a free β-gal protein which was cytoplasmic and not incorporated into virions. In contrast, the fusion protein expressed by the GBG2051 construct was readily incorporated into virions. As shown in Fig. 1B, the GBG2051 protein was expressed in Psi2 cells from the M-MuLV long terminal repeat promoter and contained M-MuLV matrix, p12, and capsid domains fused to β-gal; incorporation of this protein into virions indicated that the M-MuLV nucleocapsid domain was not required for this process.

For fine mapping of M-MuLV *gag* domains involved in assembly, we constructed 12 mutant versions of the GBG2051 construct (Fig. 1). Twelve-base-pair linker insertions at M-MuLV positions 676, 747, 919, 1074, 1084, 1436, 1560, 1672, 1752, 1862, and 1908 were generated as described in Materials and Methods and the legend to Fig. 1. These mutations were introduced into the GBG2051 construct, yielding the constructs GBG 12in 676, 747, and 919, with mutations in the matrix domain; GBG 12in 1074 and 1084, with mutations in the p12 domain; and GBG 12in 1436, 1560, 1672, 1752, 1862, and 1908, with mutations in the capsid domain (Fig. 1B). As shown in Fig. 1C, all linker insertions were expected to encode mutant proteins with four amino acids inserted plus an additional amino acid mutation in the case of GBG 12in 1672. In addition to linker insertion mutations, we transferred the previously created (31) glycine-to-alanine mutation at the second codon of M-MuLV Gag to the GBG2051 background. Since this mutation prevents myristylation, membrane association, and assembly of the wt *gag* polyprotein (31), we designated our construct GBG myr$^-$ (Fig. 1B and C).

The GBG2051, BAG, GBG myr$^-$, and all 11 GBG 12in constructs were expressed in Psi2 cells after introduction via the transfection-infection protocol of Jones et al. (17), which introduces proviral constructs into recipient cells by precise retrovirus integration rather than nonhomologous recombination, as seen in direct transfections. Our initial characterization of proteins involved quantitation of total β-gal activity in matched samples of medium released from cells (supernatant) and in cell lysates. Previous experiments

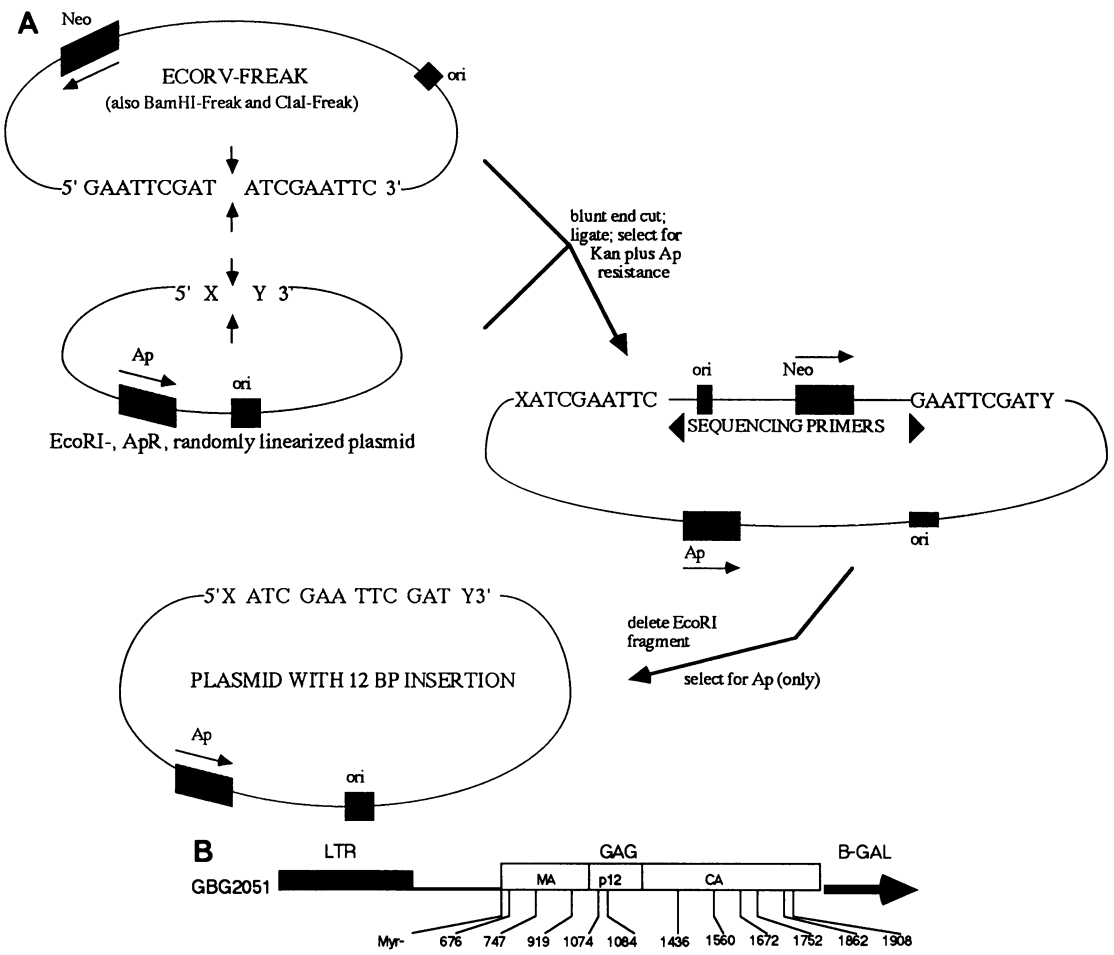

C

GBG myr-	AUG GCC CAG ACU GUU ACC ACU CCC UUA AGU
	M **G>A** Q T V T T P L S
GBG 12in676	AAA GAU GUC GAU GAA UUC AUC GAG CGG AUC
	K D V **D E F I** E R I
GBG 12in747	GCA GAA UGG AUC GAA UUC GAU CCA ACC UUU
	A E W **I E F D** P T F
GBG 12in919	CCC UUU GUA UCG AAU UCG AUA CAC CCU AAG
	P F V **S N S I** H P K
GBG 12in1074	AGU GGG GGG AUC GAA UUC GAU CCG CUC AUC
	S G G **I E F D** P L I
GBG 12in1084	CUC AUC GAU GAA UUC AUC GAC CUA CUU ACA
	L I D **E F I D** L L T
GBG 12in1436	UGU CAG CAG AUC GAA UUC GAU CUG UUG GGG
	C Q Q **I E F D** L L G
GBG 12in 1560	UUU CCC CUC GAU GAA UUC AUC GAG CGC CCA
	F P L **D E F I** E R P
GBG 12in1672	ACU AAU UUG GAU CGA AUU CGA UCC AAG GUA
	T N L **D R I R A>S** K V
GBG 12in1752	UAU CGC AGG UAU CGA AUU CGA UAC ACU CCU
	Y R R **Y R I R** Y T P
GBG 12in1862	GAA GAU UUA UCG AAU UCG AUA AAA AAC AAG
	E D L **S N S I** K N K
GBG 12in1908	GAA AAG AUC CGA AUU CGG AUC UUU AAU AAA
	E K I **R I R I** F N K

FIG. 1. M-MuLV linker insertion mutations. (A) Linker insertion mutations were generated initially in *gag* gene-containing, *Eco*RI-minus, ampicillin resistance-conferring plasmids. Target plasmids linearized with *Eco*RV-, *Cla*I-, or *Bam*HI-compatible restriction enzymes were ligated to *Eco*RV, *Cla*I, or *Bam*HI Freak plasmids. The Freak plasmids contain the designated unique restriction sites bracketed by *Eco*RI sites and possess the bacterial neomycin resistance (Neo) gene. Freak-target plasmid recombinants were selected with kanamycin (Kan) plus ampicillin (Ap), and junction regions were sequenced by using Freak-specific sequencing primers. Following analysis of junction sites, deletion of the Freak *Eco*RI fragments from Freak-target intermediates yielded target plasmids with 12-bp inserts of ATCGAATTCGAT for *Eco*RV-Freak, GATGAATTCATC for *Cla*I-Freak, and TCCGAATTCGGA for *Bam*HI-Freak. (B) Linker insertion mutations in *gag* coding regions were transferred into the GBG2051 construct for analysis. The GBG2051 construct, described previously (17), derives from the retroviral β-gal expression vector BAG (7) and expresses a protein which contains M-MuLV *gag* matrix (MA), p12, and capsid (CA) coding regions fused to β-gal. The GBG2051 Gag-β-gal fusion protein is incorporated efficiently into virions when expressed along with M-MuLV wt proteins. As shown, six CA linker insertions (GBG 12in 1436, 1560, 1672, 1752, 1862, and 1908), two p12 linker insertions (GBG 12in 1074 and 1084), and three MA linker insertions (GBG 12in 676, 747, and 919) were generated. In addition, a myristylation-minus mutation (kindly provided by A. Rein [31]) was transferred into the GBG2051 backbone, yielding the construct GBG myr$^-$. LTR, Long terminal repeat. (C) Viral RNA sequences and encoded protein sequences in mutated M-MuLV *gag* coding regions. In the case of GBG myr$^-$, the underlined mutated nucleotide corresponds to M-MuLV nt 625 (34), converting the second Gag codon from glycine to alanine and preventing myristylation (31). In the GBG 12in linker insertion mutants, the underlined nucleotide corresponds to the viral nucleotide designated by the construct name. Inserted amino acid residues are indicated in boldface letters; mutations which change amino acid residues (glycine to alanine, G>A; alanine to serine, A>S) are also shown in boldface type.

showed that normalization for total cellular protein and/or total reverse transcriptase activity in the supernatant did not alter relative ratios (17). As shown in Table 1, the free β-gal produced from the BAG construct was not released from cells, as demonstrated by a supernatant-to-cell β-gal ratio of

0.016. In contrast, the fusion protein produced by the GBG2051 construct gave a ratio of 0.482, indicating that it was released from cells at a high rate. These results were comparable to those in our previous studies, which gave ratios of 0.017 and 0.567 for BAG and GBG2051, respectively (17).

Analysis of our 12 mutant constructs indicated that only the three most amino-terminal mutations (GBG myr$^-$, GBG 12in 676, and GBG 12in 747) prohibited release of β-gal activity from cells. All other linker insertion mutants (GBG 12in 919 and longer) expressed proteins that were released from cells at levels comparable to that of the GBG2051 parental construct and at least 10 times higher than free β-gal produced by the BAG construct. In general, these results corroborate our previous results (17), indicating that determinants necessary for fusion protein release from cells are contained within the M-MuLV matrix domain. One minor disparity is that the GBG 12in 919 Gag-β-gal protein was released from cells (supernatant/cell β-gal ratio, 0.596), while our previous studies (17) indicated that a Gag-β-gal protein fused at nt 917 (construct GBG917) was not released from cells (ratio, =0.005). This discrepancy could be caused by insertion of nondisruptive amino acids in the GBG 12in 919 construct or by disruption of neighboring matrix protein domains when β-gal is fused directly to the carboxy-terminal region of matrix in the GBG917 construct.

While our previous work indicated that supernatant and cellular β-gal activity levels reflected protein levels (17), release of β-gal activity from cells does not necessarily indicate that fusion proteins are incorporated into virions. Indeed, the GBG2051 protein was released from cells in two forms: one is a virus-associated high-density form, and the other is associated with a low-density membrane vesicle form (17). Thus, in order to determine whether supernatant Gag-β-gal proteins were in virions, it was necessary to fractionate supernatant material on sucrose density gradients.

Figure 2 illustrates the results of our density fractionations on all GBG 12in proteins that were released from cells. As shown, our marker for virus particles, reverse transcriptase activity, fractionated to the bottom of our gradients, at a density of 1.15 to 1.16 g/ml. Fusion constructs GBG 12in 919, 1074, 1084, and 1908 produced Gag-β-gal proteins that fractionated similarly to the GBG2051 protein; 30 to 80% of the released β-gal activity was virion associated, while the remainder was in the light-density fraction. However, constructs with mutations in the amino-terminal portions of the capsid region (GBG 12in 1436 through 1862) expressed proteins that, for the most part, were excluded from virus particles. These results suggest that interactions involving the amino-terminal two-thirds of the capsid domains are required for protein assembly into virions.

Subcellular localization of Gag-β-gal proteins. Why were matrix mutant fusion proteins not released from cells? To answer this question, we examined the subcellular localization of proteins produced by BAG, GBG2051, and all matrix mutants. Our method was to measure β-gal activities in crude membrane (P2) and cytosol (S2) fractions (10) of cell lysates (Fig. 3). Not surprisingly, virtually all of the free β-gal produced by the BAG construct fractionated to the cytosol, while over two-thirds of the Gag-β-gal from the GBG2051 construct was membrane associated (Table 2). On the basis of specific activities, the GBG2051 protein was 70-fold enriched in membranes relative to free β-gal. The GBG 12in 919 protein, which was efficiently released from cells and incorporated into virions, also fractionated to cellular membranes. However, the GBG myr$^-$, 12in 676, and 12in 747 proteins had reduced levels of membrane association. The GBG 12in 747 protein, which had an insert at residue 42 of the myristylated matrix domain, was reduced twofold in its membrane affinity relative to the wt GBG2051 protein but still partitioned over half of its β-gal activity to the P2 fraction. The GBG myr$^-$ and 12in 676 proteins were largely cytosolic, although their levels of membrane association were slightly higher (two- to fourfold) than that of free β-gal.

TABLE 1. B-Gal released from cells[a]

Construct	β-Gal activity ratio, supernatant/cell
BAG	0.016 ± 0.009
GBG myr$^-$	0.011
GBG 12in 676	0.020 ± 0.023
GBG 12in 747	0.049 ± 0.020
GBG 12in 919	0.596 ± 0.415
GBG 12in 1074	1.49
GBG 12in 1084	0.671
GBG 12in 1436	0.632 ± 0.245
GBG 12in 1560	0.356
GBG 12in 1672	0.327
GBG 12in 1752	0.202 ± 0.067
GBG 12in 1862	0.437 ± 0.182
GBG 12in 1908	0.570
GBG2051	0.482 ± 0.226

[a] Confluent Psi2 cells expressing each recombinant construct were split 1:20 or 1:40 into 10-cm tissue culture plates and grown for 48 to 72 h. Supernatant medium (10 ml) was collected, filtered through a 0.45-μm-pore-size filter, pelleted at 4°C for 2 to 4 h at 274,000 × *g* (SW41 rotor at 40,000 rpm), and suspended in phosphate-buffered saline (PBS) before enzyme assay. Cells were washed twice with PBS, scraped from plates into 1 ml of PBS, pelleted in a microcentrifuge, and resuspended in PBS. Enzyme assays on cell and supernatant samples were performed as described previously (17). From these, total cell and supernatant β-gal activities were calculated. Results are expressed as the ratio of total enzyme activity in the supernatant sample versus the cell sample, with standard deviations indicated when possible. BAG values are from five independent trials; GBG2051 and GBG 12in 747, 919, 1436, 1752, and 1862 values are from three trials each; GBG 12in 676 values are from two experiments; all other values are from one experiment.

Since the above fractionation experiments implied altered subcellular localization patterns for proteins with mutations in the *gag* matrix domain, we performed immunofluorescence studies to visualize these patterns. Figure 4 shows examples of our β-gal and Gag-β-gal immunofluorescence localization studies. As illustrated, free β-gal was present throughout cells expressing the BAG construct, although the protein was reduced somewhat in cell nuclei (Fig. 4A). In contrast, the GBG 12in 919 protein stained a heterogeneous perinuclear area as well as a microfilamentous region at the cell periphery (Fig. 4D); this pattern was similar to that seen with the GBG2051 protein (17) (see also Fig. 6C). Due to low expression levels, we were unable to perform immunofluorescence studies on the GBG 12in 676 protein. However, our results with the GBG myr$^-$ mutant protein (Fig. 4B), as anticipated (31), gave a cytoplasmic staining pattern similar to that of free β-gal, with little, if any, nuclear staining. Interestingly, the GBG 12in 747 protein yielded a perinuclear staining pattern (Fig. 4C) that suggested that the protein was trapped on intracellular membranes (12, 22, 32). This pattern was different from the staining pattern we obtained when staining the Golgi apparatus with FITC-conjugated wheat germ agglutinin. While the Golgi appeared as a flattened disk of fluorescence on one side of the cell nucleus, the GBG 12in 747 protein formed a diffuse rosette around the entire nu-

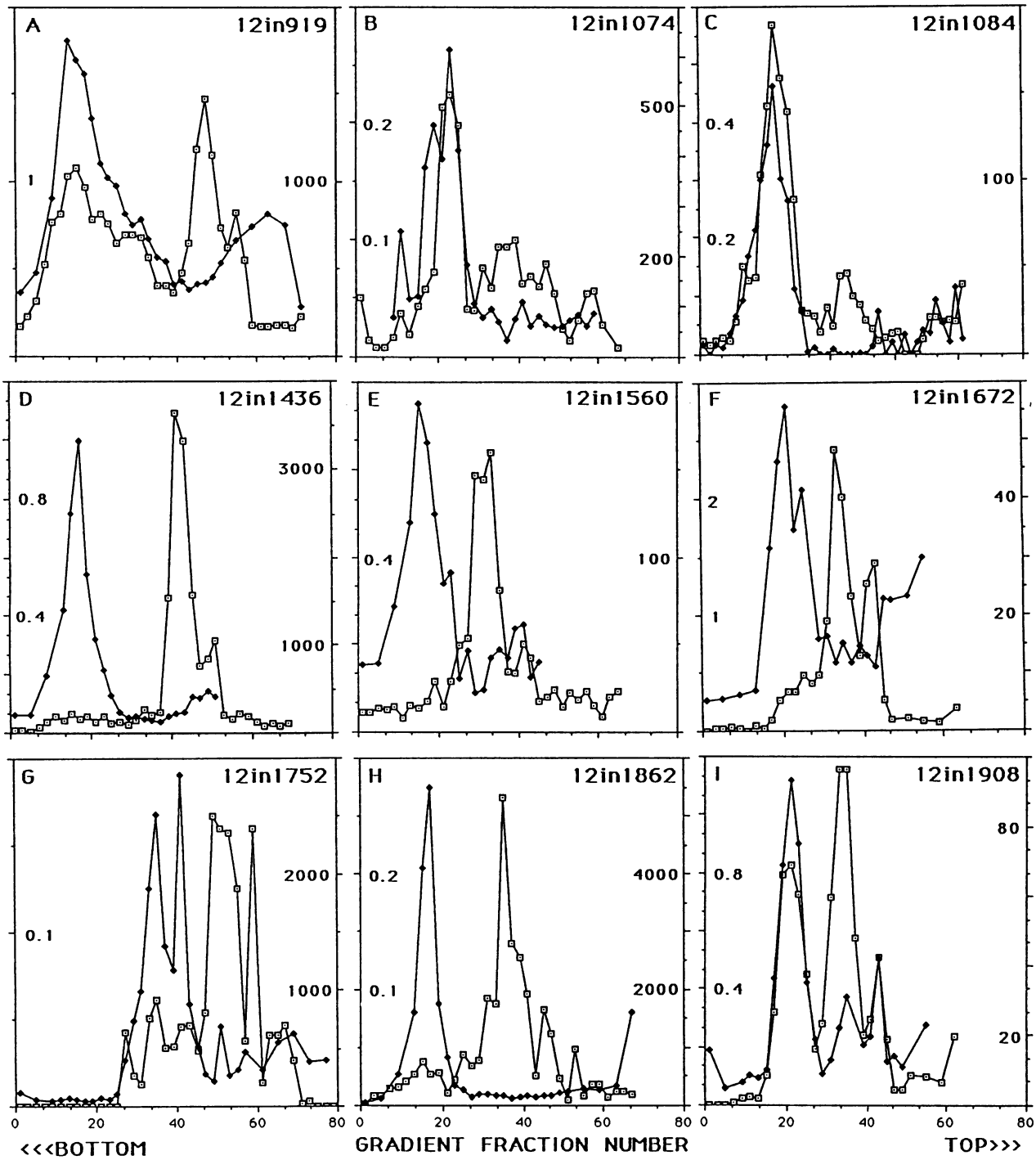

FIG. 2. Sucrose density gradient fractionation of supernatant material. Supernatant material from cells expressing the indicated constructs was fractionated by sucrose density gradient centrifugation (20 to 50% gradients) as described in Materials and Methods. Fractions (0.5 ml) were collected from the bottom of the gradients, and fraction densities, β-gal activities (□), and reverse transcriptase activities (◆) were determined. In each gradient, the bottom of the gradient is at the left, β-gal activities are in units per fraction on each left vertical axis and reverse transcriptase activities are in counts per minute of incorporated [^{32}P]dTTP per 10 μl on each right vertical axis. When densities were determined (panels A, C, D, F, G, H, and I), reverse transcriptase peaks were at densities of 1.15 to 1.16 g/ml and light-density β-gal peaks were at 1.11 to 1.13 g/ml.

cleus. Experiments concerning the interpretation of the GBG 12in 747 staining pattern are described below.

Inhibition of Gag and Gag-β-gal transport by monensin. Although we did not assess the myristylation status of the GBG myr$^-$ or 12in proteins in these studies, our previous work (17) and that of others (6, 18, 20, 31) would indicate that the GBG 12in proteins should be myristylated and that the glycine-to-alanine mutation of GBG myr$^-$ should pre-

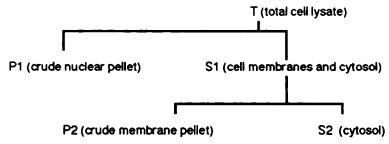

FIG. 3. Membrane fractionation protocol.

vent myristylation. Likewise, our previous work suggests that variant glycosylated Gag-β-gal proteins (1, 11, 30, 39), if present, should represent a minor fraction of the Gag-β-gal proteins in our study (17). Thus, we believe that the GBG 12in 747 protein is trapped at intracellular membranes not because it is modified inappropriately, but as a direct consequence of its linker insertion mutation. The aberrant localization of GBG 12in 747 (and the GBG 12in 648, 730, and 917 proteins in our previous study [17]) suggests two possibilities. First, the localization may reflect an unnatural missorting of a mutant protein. Alternatively, the GBG 12in 747 protein may be blocked at a stage in the natural routing of viral *gag* proteins via vesicular transport to the cell surface. Assuming that this latter hypothesis is true, it should be possible to inhibit transport of *gag* proteins by inhibition of intracellular vesicular transport. To test this prediction, we examined the effect of monensin, an inhibitor of vesicular transport, on the process of M-MuLV particle assembly.

Initially, we decided to assess the effects of monensin on the release of reverse transcriptase and β-gal activity from Psi2 cells expressing the Gag-β-gal GBG2051 protein, which is efficiently incorporated into M-MuLV virions (see above). Control experiments indicated that treatment of cells with 25 μM monensin for up to 9 h had no apparent effect on cell morphology or total cell protein levels (data not shown). However, in both subconfluent and confluent cells, release of reverse transcriptase activity from treated cells was reduced approximately ninefold, while β-gal release was reduced two- to sevenfold (Table 3). We have not established whether concentrations below 25 μM monensin will inhibit M-MuLV reverse transcriptase release, but our results indicate that 10 μM monensin is adequate for inhibition of Gag-β-gal release (Table 3). Immunofluorescence experiments also indicate that 10 μM monensin inhibits intracellular transport of Gag-β-gal proteins (see below).

Although our initial results indicated that release of reverse transcriptase activity from M-MuLV-producing cells was inhibited by monensin, these experiments did not show conclusively that monensin acts by transport blockage of the reverse transcriptase precursor Pr180$^{gag\text{-}pol}$. For direct measurement of Gag levels, Psi2 cells expressing only wt M-MuLV proteins were collected after mock or monensin treatment. Matched medium supernatants from experimental cells were centrifuged at 4°C for 30 min at 274,000 × *g* to pellet virus particles. Proteins in cell lysates and virus pellets were subjected to polyacrylamide gel electrophoresis and electroblotted onto a nitrocellulose membrane. Afterwards, p12^{gag}, capsid (p30), and envelope-related viral proteins were visualized by successive rounds of immunodetection. Our results (Fig. 5) on three separate sets of mock- and monensin-treated cells showed that cellular Pr65^{gag} levels were not affected by monensin treatment (compare lanes g and h, i and j, and k and l). However, clear differences in virus-associated *gag* protein levels were detected. Specifically, supernatants from monensin-treated cells had reduced amounts of p30^{gag} and p12^{gag} relative to those from mock-treated cells (Fig. 5, lanes a and b; c and d; e and f). We estimate these differences to be three- to fivefold. In all monensin-treated-cell supernatants, Pr65^{gag} was present at higher levels than in mock-treated cell supernatants, probably reflecting a monensin effect on precursor processing (see below). Nevertheless, as Pr65^{gag} was a minor constituent in viral samples relative to p30 and p12, our data suggest that monensin treatment inhibits *gag* protein release from cells.

Our positive control for sensitivity to monensin was the M-MuLV envelope protein, an integral membrane protein whose transport should be inhibited by monensin (5, 41). While total cellular levels of envelope proteins (Pr80^{env} plus gp70) were relatively unaffected by monensin treatment (Fig. 5, lanes g to l), monensin-treated-cell supernatants (Fig. 5, lanes a to f) were reduced 5- to 10-fold in envelope protein levels relative to mock-treated-cell supernatants. These results suggest that, while inhibited by monensin, Gag release from cells is somewhat less sensitive to treatment than envelope protein release. Another point is that Pr80^{env} processing, like that of Pr65^{gag}, was inhibited by treatment. Monensin-treated cells and supernatants had higher ratios of Pr80^{env} to mature gp70 than did mock-treated cells and supernatants, supporting the observation that processing is transport dependent (5, 42). Of additional interest were minor 28- and 25-kDa Gag-related proteins of unknown origin (Fig. 5, black dots) which were reduced in abundance in treated cells (25-kDa protein) and supernatants (28-kDa protein). The significance of these minor species and the p12^{gag}-related 27-kDa protein present in all viral supernatants (possibly an unprocessed matrix-p12 polypeptide) is presently unclear.

The results described above indicate that monensin inhibits release of reverse transcriptase activity, Gag-β-gal activity, and wt *gag* proteins from cells. While some of these effects may be attributable to blocked precursor processing, reduced capsid and p12^{gag} levels in treated supernatants (Fig. 5) implied that direct effects on release were involved. Since it was conceivable that drug treatment might block either transport to the plasma membrane or assembly and release of virions at the plasma membrane, we examined the subcellular distributions of Gag and GBG2051 Gag-β-gal proteins after monensin or mock treatment. Wt *gag* protein (presumably Pr65^{gag}) in untreated Psi2 cells detected with an anti-p12^{gag} antibody stained in a heterogeneous pattern extending to peripheral cellular projections, with slightly enhanced fluorescence around the nucleus (Fig. 6A). The GBG2051 Gag-β-gal protein demonstrated a roughly similar pattern (Fig. 6C), with more noticeable staining of the cell

TABLE 2. Membrane association of proteins[a]

Construct in Psi2 cells	β-Gal activity ratio, P2/S2	β-Gal sp act ratio, P2/S2
BAG	0.025 ± 0.010	0.359 ± 0.227
GBG myr$^-$	0.143 ± 0.087	1.49 ± 1.44
GBG 12in 676	0.092 ± 0.031	0.734 ± 0.379
GBG 12in 747	1.40 ± 1.05	8.36 ± 4.75
GBG 12in 919	2.35	29.8
GBG2051	2.76 ± 1.84	25.7 ± 17.3

[a] Membrane association of proteins was monitored by crude cell fractionation (10) into a crude membrane fraction, P2, and a cytosolic fraction, S2 (see Fig. 3). Proteins were expressed from the indicated constructs in Psi2 cells. Fractions were assayed for β-gal activity (28) and protein (24). Ratios of total membrane (P2) versus cytosol (S2) activities are shown, along with standard deviations. GBG2051 values are from four independent trials; BAG values are from three trials; GBG myr$^-$, GBG 12in 676, and GBG 12in 747 results are from two experiments each; GBG 12in 919 values are from one experiment.

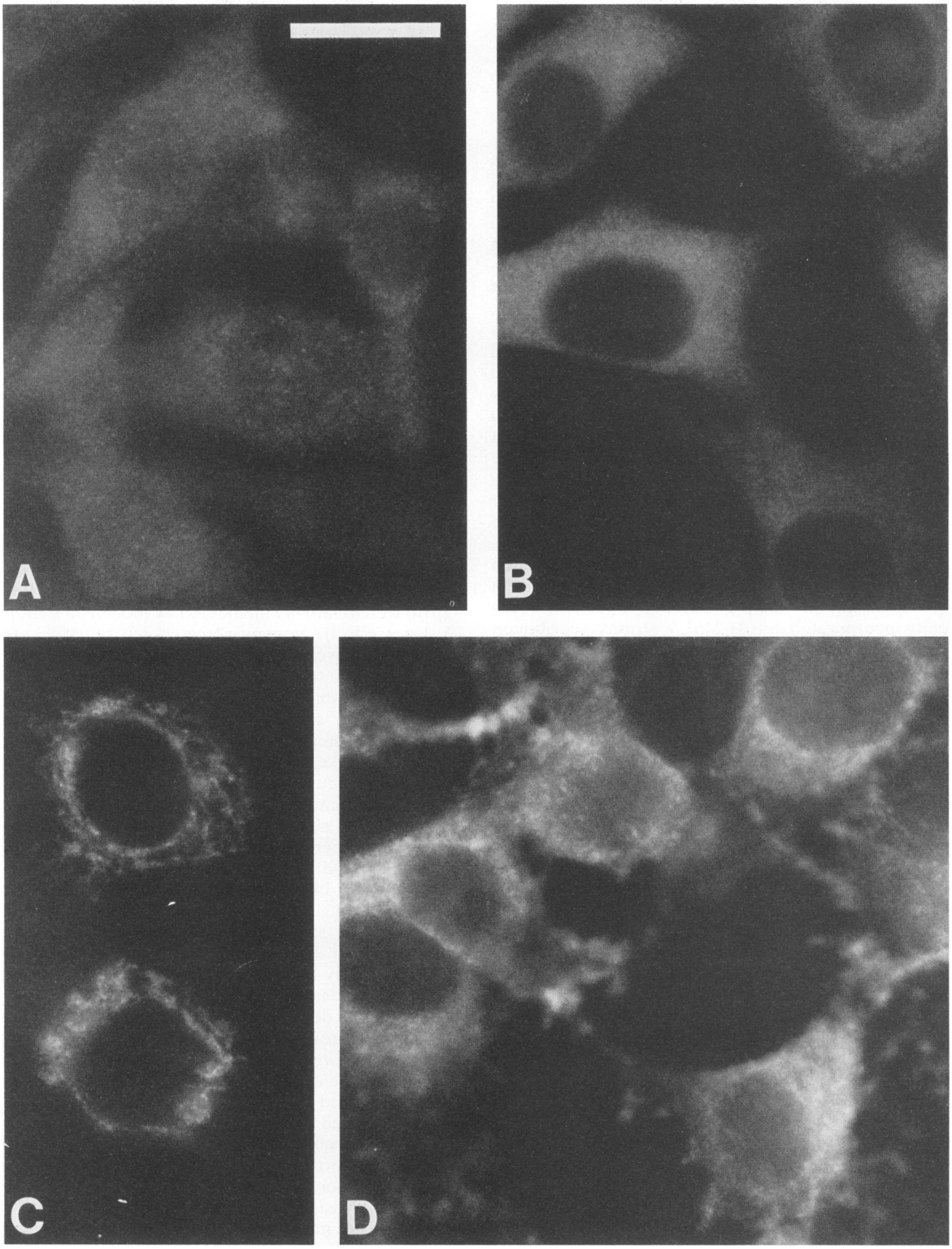

FIG. 4. Indirect immunofluorescence detection of β-gal and Gag-β-gal fusion proteins in cells. Cells grown on cover slips were fixed, permeabilized, and subjected to indirect immunofluorescence analysis with mouse anti-β-gal antibody as the primary reagent, followed by rhodamine-conjugated goat anti-mouse IgG antibody (see Materials and Methods). Bar, 20 μm. All photographs are of proteins expressed in Psi2 cells. (A) BAG; (B) GBG myr$^-$; (C) GBG 12in 747; (D) GBG 12in 919.

TABLE 3. Enzyme activity released after monensin treatment[a]

Psi2 cells	Monensin treatment			RT activity (U)		RT activity ratio, mock/monensin	β-Gal activity (U)			β-Gal activity in supernatant, ratio, mock/monensin
	Concn (μM)	Duration (h)		Supernatant	Normalized		Supernatant	Cells	Normalized, supernatant	
		Pretreatment	Incubation							
50% confluent	0 (mock)	3	6	36.8	36.8		37.1	312.4	37.1	
	25	3	6	3.9	4.1	9.0	5.7	299.8	5.9	6.3
Confluent	0 (mock)	3	6	346.0	346.0		61.8	558.6	61.8	
	25	3	6	22.7	37.1	9.3	14.8	340.9	24.3	2.5
Confluent	0 (mock)	1	5				27.6	193.8	27.6	
	10	1	5				10.3	220.4	9.1	3.0
	25	1	5				9.9	209.0	9.2	3.0

[a] Plates (10 cm) of Psi2 cells expressing wt M-MuLV proteins as well as the GBG2051 construct were mock treated or treated with 10 or 25 μM monensin as indicated. Treatments consisted of a 1-h or 3-h pretreatment with the indicated amount of monensin, followed by a 5-h or 6-h incubation with monensin. Following treatments, supernatant medium was collected, pelleted, and suspended as described in Table 1, footnote *a*, prior to enzyme assays. Cells were collected for β-gal assays as described in Table 1, footnote *a*. Total units of supernatant reverse transcriptase (RT) activities were determined as described in Materials and Methods, with dilutions of purified avian myeloblastosis virus reverse transcriptase as standards. Total units of supernatant and cellular β-gal activities were determined as described in Table 1, footnote *a*. Total enzyme activities in treated supernatants were normalized by multiplication to a normalization factor (total cellular β-gal activity in treated versus mock-treated cells) to account for monensin effects on myristylated fusion proteins in cells. Ratios of normalized supernatant enzyme activities from treated versus mock-treated cells provide a rough estimate of the effect of monensin treatment on enzyme activity release.

periphery and perinuclear region. Cells treated with 25 μM (Fig. 6B and D) or 10 μM (Fig. 6E) monensin showed different patterns. Both Gag (Fig. 6B) and Gag-β-gal (Fig. 6D and E) proteins localized to a perinuclear region in a distinct punctate pattern; peripheral regions remained unstained. The localization patterns of *gag*-related proteins in monensin-treated cells were similar to those seen for intracellularly trapped mutant Gag-β-gal proteins (17) (Fig. 4C) and suggest that a significant proportion of M-MuLV *gag* proteins travel to the cell surface via vesicular transport. That these were myristylated *gag* proteins and not the variant glycosylated Gag (1, 11, 30, 39) is strongly supported by the fact that the glycosylated *gag* initiation codon (30) and leader region are deleted in the Psi2 construct (26).

DISCUSSION

We have studied the process of M-MuLV *gag* protein assembly into M-MuLV particles by using both mutants and the ionophore monensin. Our method has been to assess virion incorporation of *gag* proteins or mutants of the GBG2051 Gag-β-gal fusion protein, which is ordinarily targeted into virions (17). In support of previous experiments (17, 31), our current studies indicate that mutations in the amino-terminal portion of the *gag* matrix domain prohibit protein release from cells (Table 1; GBG myr$^-$ and GBG 12in 676 and 747). These proteins had reduced affinities to cellular membranes (Table 2) and were either cytoplasmically localized or trapped on intracellular membranes (Fig.

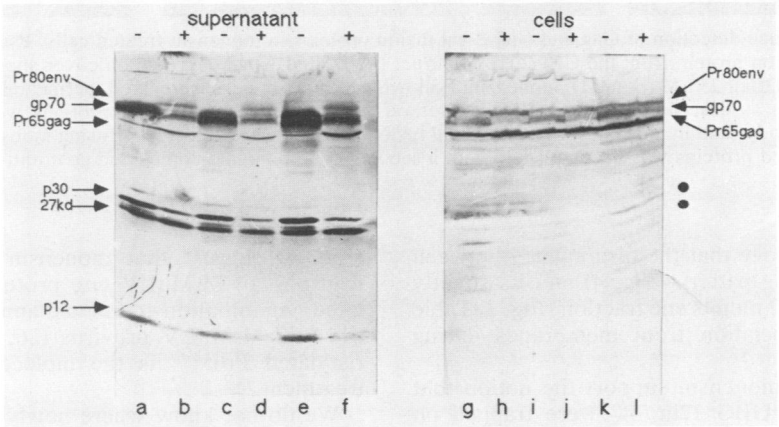

FIG. 5. Effect of monensin on release of *gag* and envelope proteins from cells. Matched 10-cm plates of Psi2 cells at 50% (lanes a, b, g, h), 75% (lanes c, d, i, j), and 100% (lanes e, f, k, l) confluence were mock treated (−, lanes a, c, e, g, i, k) or treated with 25 μM monensin for 3 h, washed, and then incubated for 6 h with monensin (+, lanes b, d, f, h, j, l). Following treatments, cell lysates were collected as described in Materials and Methods. Virus particles in supernatants were collected by filtration through a 0.45-μm-pore-size filter, followed by centrifugation at 4°C for 30 min at 274,000 × *g* (SW41 rotor at 40,000 rpm) through a 2-ml cushion of 20% sucrose in PBS. Supernatant samples (lanes a to f; corresponding to 50% of the total sample) and cell samples (lanes g to l; corresponding to 10% of the total cell sample) were subjected to sodium dodecyl sulfate-polyacrylamide gel electrophoresis and electroblotted onto a nitrocellulose filter. M-MuLV proteins were detected immunologically with anti-viral protein antibodies, followed by secondary alkaline phosphatase-conjugated antibodies and detection of alkaline phosphatase activity. Three successive rounds of protein detection were done with differing primary antibodies in the following order: mouse anti-p12^{gag} monoclonal, mouse anti-p30^{gag} monoclonal, and goat anti-feline leukemia virus gp71 polyclonal. Viral Pr80^{env}, gp70^{env}, Pr65^{gag}, p30^{gag} (capsid), and p12^{gag} proteins are indicated. A 27-kDa protein detected in supernatant samples with the anti-p12^{gag} antibody is also indicated (27 kd). Black dots additionally show minor 28- and 25-kDa *gag*-related proteins of unknown origin which were reduced in abundance in treated cells (25-kDa protein) and supernatants (28-kDa protein). Supernatant and cell samples on filters were processed separately for immunodetection.

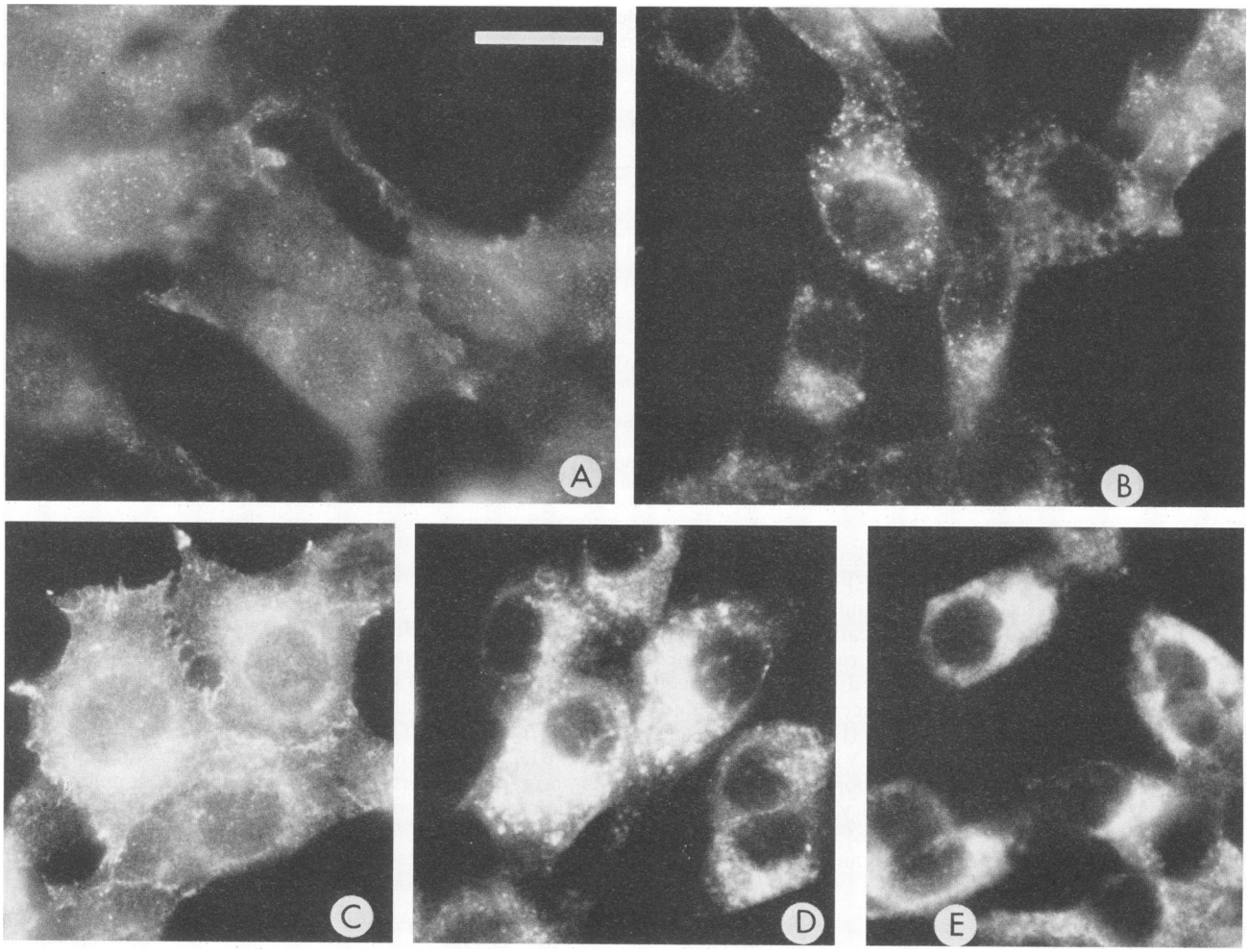

FIG. 6. Immunofluorescence detection of Gag and Gag-β-gal fusion proteins in monensin-treated cells. Psi2 cells (A and B) or Psi2 cells expressing the Gag-β-gal fusion protein from the GBG2051 construct (C, D, and E) were grown on cover slips and mock treated (A and C) or treated for 4 h with 10 μM (E) or 25 μM (B and D) monensin. Following treatment, cells were fixed, permeabilized, and subjected to indirect immunofluorescence analysis as described in Materials and Methods. In panels A and B, *gag* proteins were detected by using mouse anti-p12^{gag} monoclonal antibody, and in panels C to E, Gag-β-gal fusion proteins were detected by using mouse anti-β-gal antibody. In each case, visualization of localized proteins was accomplished with a secondary, rhodamine-conjugated goat anti-mouse IgG antibody. Bar, 20 μm.

4). In this regard, we believe that the discrepancy between the GBG 12in 747 staining pattern (Fig. 4) and its slightly reduced retention in the P2 membrane fraction (Fig. 3, Table 2) may be due to dissociation from membranes during fractionation.

Our experiments with monensin support the notion that mutant proteins such as GBG 12in 747 were trapped on intracellular membranes that are on the normal Gag transport route to the cell surface. Monensin, which blocks vesicular transport of newly synthesized transmembrane proteins at the Golgi apparatus (5, 16, 19, 38), clearly reduced release of reverse transcriptase and Gag-β-gal activities from treated cells (Table 3). Almost certainly, part of this activity release inhibition was due to impaired precursor processing. However, direct assay of cell and supernatant Gag levels in mock- and monensin-treated cells showed a reduction of released p12^{gag} and p30^{gag} proteins from treated cells (Fig. 5). This result and the observation that monensin treatment resulted in an accumulation of wt Gag and GBG2051 Gag-β-gal proteins to a perinuclear region (Fig. 6) suggest that monensin inhibits the intracellular transport of M-MuLV *gag* proteins. Because the glycosylated *gag* initiation codon and amino terminus are deleted in the Psi2 M-MuLV provirus (26, 30), we believe that myristylated Pr65^{gag} is the molecule affected by monensin treatment.

We do not know where newly synthesized and myristylated *gag* proteins first become membrane associated. No obvious rough endoplasmic reticulum or Golgi staining pattern was apparent either with the GBG 12in 747 protein (Fig. 4) or with *gag* proteins in monensin-treated cells (Fig. 6). Until detailed subcellular fractionation studies prove otherwise, we consider it possible that myristylated *gag* proteins associate with a variety of intracellular membranes prior to cell surface routing. We also consider it feasible that some Pr65^{gag} travels freely through the cytoplasm to the plasma membrane. This possibility, suggested by the differential effect of monensin on Gag and envelope protein release from cells (Fig. 5), may explain the inability of monensin to completely block retrovirus assembly (5) and relate to the

partial effect of human immunodeficiency virus *vpu* mutations on virus budding (21, 36, 37).

Regardless of the Gag pathway to the plasma membrane, our mutant studies demonstrate the importance of Gag capsid determinants in M-MuLV particle formation. It is clear that linker insertions into the capsid domain of GBG2051 did not inhibit fusion protein release from cells (Table 1). However, five of six capsid linker insertion mutations (GBG 12in 1436, 1560, 1672, 1752, and 1862) blocked fusion protein assembly into virions, permitting release only in the low-density, presumably plasma membrane vesicle-derived fraction (Fig. 2). The one capsid mutation which did not affect fusion protein assembly into virions was GBG 12in 1908, an insertion of charged amino acid residues preceding the highly charged carboxy terminus of the capsid domain (Fig. 1C). Either this is a neutral mutation for M-MuLV, or it affects some other aspect of the viral life cycle; further experimentation with replication-competent constructs may distinguish between these alternatives.

In addition to the GBG 12in 1908 mutant, three other mutants, GBG 12in 919, 1074, and 1084 also did not eliminate Gag-β-gal assembly into virions. As noted for GBG 12in 1908, these mutations may also be neutral for M-MuLV. Alternatively, these mutations may influence viral functions other than assembly. Indeed, Crawford and Goff (9) have found that deletions of as many as 144 nt at the M-MuLV matrix-p12 border (M-MuLV nt 944 to 1088) do not impair virus assembly. However, such mutations resulted in the formation of mutant virions which were blocked at an early step of infection, possibly at the uncoating stage (9). It will be of interest to determine whether our linker insertions demonstrate similar phenotypes when transferred to M-MuLV proviral constructs.

ACKNOWLEDGMENTS

We thank Thomas Jones, David Kabat, Geraldine Kempler, Catharine Mace, Richard Petersen, and Milton Yatvin for helpful advice and discussions.

This work was supported by grant 5-661 from the March of Dimes Birth Defects Foundation and by Public Health Service grant 5R01 CA47088-02 from the National Cancer Institute.

LITERATURE CITED

1. **Arcement, L., W. Karshin, R. Naso, G. Jamjoom, and R. Arlinghaus.** 1976. Biosynthesis of Rauscher leukemia viral proteins: presence of p30 and envelope p15 sequences in precursor polypeptides. Virology **69**:763–774.
2. **Barbacid, M., J. Stephenson, and S. Aaronson.** 1976. *gag* gene of mammalian type-C RNA tumour viruses. Nature (London) **262**:554–559.
3. **Barklis, E., R. Mulligan, and R. Jaenisch.** 1986. Chromosomal position or virus mutation permits retrovirus expression in embryonal carcinoma cells. Cell **47**:391–399.
4. **Bolognesi, D., R. Luftig, and J. Shaper.** 1973. Localization of RNA tumor virus polypeptides. I. Isolation of further virus substructures. Virology **56**:549–564.
5. **Bosch, J., and R. Schwarz.** 1984. Processing of gPr92^{env}, the precursor to the glycoproteins of Rous sarcoma virus: use of inhibitors of oligosaccharide trimming and glycoprotein transport. Virology **132**:95–109.
6. **Buss, J. E., C. J. Der, and P. A. Solski.** 1988. The six amino-terminal amino acids of p60^{src} are sufficient to cause myristylation of p21$^{v\text{-}ras}$. Mol. Cell. Biol. **8**:3960–3963.
7. **Cepko, C., B. Roberts, and R. Mulligan.** 1984. Construction and applications of a highly transmissible murine retrovirus shuttle vector. Cell **37**:1053–1062.
8. **Chesebro, B., W. Britt, L. Evans, K. Wehrly, J. Nishio, and M. Cloyd.** 1983. Characterization of monoclonal antibodies reactive with murine leukemia viruses: use in analysis of strains of Friend MCF and Friend ecotropic murine leukemia virus. Virology **127**:134–148.
9. **Crawford, S., and S. P. Goff.** 1984. Mutations in *gag* proteins P12 and P15 of Moloney murine leukemia virus block early stages of infection. J. Virol. **49**:909–917.
10. **Dickson, C., and M. Atterwill.** 1980. Structure and processing of the mouse mammary tumor virus glycoprotein precursor Pr73^{env}. J. Virol. **35**:349–361.
11. **Edwards, S. A., and H. Fan.** 1979. *gag*-related polyproteins of Moloney murine leukemia virus: evidence for independent synthesis of glycosylated and unglycosylated forms. J. Virol. **30**:551–563.
12. **Gething, M., K. McCammon, and J. Sambrook.** 1986. Expression of wild-type and mutant forms of influenza hemagglutinin: the role of folding in intracellular transport. Cell **46**:939–950.
13. **Goff, S., P. Traktman, and D. Baltimore.** 1981. Isolation and properties of Moloney murine leukemia virus mutants: use of a rapid assay for release of virion reverse transcriptase. J. Virol. **38**:239–248.
14. **Hanafusa, H., D. Baltimore, D. Smoler, K. Watson, A. Yaniv, and S. Spiegelman.** 1972. Absence of polymerase protein in virions of alpha-type Rous sarcoma virus. Science **177**:1188–1191.
15. **Henderson, L., H. Krutzsch, and S. Oroszlan.** 1983. Myristyl amino-terminal acylation of murine retrovirus proteins: an unusual post-translational protein modification. Proc. Natl. Acad. Sci. USA **80**:339–343.
16. **Johnson, D., and M. Schlesinger.** 1980. Vesicular stomatitis virus and Sindbis virus glycoprotein transport to the cell surface is inhibited by ionophores. Virology **103**:407–424.
17. **Jones, T., G. Blaug, M. Hansen, and E. Barklis.** 1990. Assembly of *gag*-β-galactosidase proteins into retrovirus particles. J. Virol. **64**:2265–2279.
18. **Jørgensen, E. C., N. O. Kjeldgaard, F. S. Pedersen, and P. Jørgensen.** 1988. A nucleotide substitution in the *gag* N terminus of the endogenous ecotropic DBA/2 virus prevents Pr65^{gag} myristylation and virus replication. J. Virol. **62**:3217–3223.
19. **Kaariainen, L., K. Hashimoto, J. Saraste, I. Virtanen, and K. Penttinen.** 1980. Monensin and FCCP inhibit the intracellular transport of alphavirus membrane glycoproteins. J. Cell Biol. **87**:783–791.
20. **Kaplan, J. M., G. Mardon, J. M. Bishop, and H. E. Varmus.** 1988. The first seven amino acids encoded by the v-*src* oncogene act as a myristylation signal: lysine 7 is a critical determinant. Mol. Cell. Biol. **8**:2435–2441.
21. **Klimkait, T., K. Strebel, M. D. Hoggan, M. A. Martin, and J. M. Orenstein.** 1990. The human immunodeficiency virus type 1-specific protein *vpu* is required for efficient virus maturation and release. J. Virol. **64**:621–629.
22. **Kreis, T., and H. Lodish.** 1986. Oligomerization is essential for transport of vesicular stomatitis viral glycoprotein to the cell surface. Cell **46**:929–937.
23. **Levin, J. G., P. M. Grimley, J. M. Ramseur, and I. K. Berezesky.** 1974. Deficiency of 60 to 70*S* RNA in murine leukemia virus particles assembled in cells treated with actinomycin D. J. Virol. **14**:152–161.
24. **Lowry, O. H., N. J. Rosebrough, A. L. Farr, and R. J. Randall.** 1951. Protein measurement with the Folin phenol reagent. J. Biol. Chem. **193**:265–275.
25. **Maniatis, T., E. F. Fritsch, and J. Sambrook.** 1982. Molecular cloning: a laboratory manual. Cold Spring Harbor Laboratory, Cold Spring Harbor, N.Y.
26. **Mann, R., R. Mulligan, and D. Baltimore.** 1983. Construction of a retrovirus packaging mutant and its use to produce helper-free defective retrovirus. Cell **33**:153–159.
27. **Miller, A. D., and C. Buttimore.** 1986. Redesign of retrovirus packaging cell lines to avoid recombination leading to helper virus production. Mol. Cell. Biol. **6**:2895–2902.
28. **Norton, P. A., and J. M. Coffin.** 1985. Bacterial β-galactosidase as a marker of Rous sarcoma virus gene expression and replication. Mol. Cell. Biol. **5**:281–290.
29. **Oroszlan, S., L. Henderson, J. Stephenson, T. Copeland, C.**

Long, J. Ihle, and R. Gilden. 1978. Amino- and carboxyl-terminal amino acid sequences of proteins coded by *gag* gene of murine leukemia virus. Proc. Natl. Acad. Sci. USA **75**:1404–1408.

30. **Prats, A., G. De Billy, P. Wang, and J. Darlix.** 1989. CUG initiation codon used for the synthesis of a cell surface antigen coded by the murine leukemia virus. J. Mol. Biol. **205**:363–372.
31. **Rein, A., M. McClure, N. Rice, R. Luftig, and A. Schultz.** 1986. Myristylation site in $Pr65^{gag}$ is essential for virus particle formation by Moloney murine leukemia virus. Proc. Natl. Acad. Sci. USA **83**:7246–7250.
32. **Rose, J., and J. Bergmann.** 1983. Altered cytoplasmic domains affect intracellular transport of the vesicular stomatitis virus glycoprotein. Cell **34**:513–524.
33. **Shields, A., O. Witte, E. Rothenberg, and D. Baltimore.** 1978. High frequency of aberrant expression of Moloney murine leukemia virus in clonal infections. Cell **14**:601–609.
34. **Shinnick, T., R. Lerner, and J. Sutcliffe.** 1981. Nucleotide sequence of Moloney murine leukaemia virus. Nature (London) **293**:543–548.
35. **Stephenson, J., S. Tronick, and S. Aaronson.** 1975. Murine leukemia virus mutants with temperature-sensitive defects in precursor processing cleavage. Cell **6**:543–548.
36. **Strebel, K., T. Klimkait, F. Maldarelli, and M. A. Martin.** 1989. Molecular and biochemical analyses of human immunodeficiency virus type 1 *vpu* protein. J. Virol. **63**:3784–3791.
37. **Strebel, K., T. Klimkait, and M. Martin.** 1988. A novel gene of HIV-1, *vpu*, and its 16-kilodalton product. Science **241**:1221–1223.
38. **Tartakoff, A.** 1983. Perturbation of vesicular traffic with the carboxylic ionophore monensin. Cell **32**:1026–1028.
39. **Tung, J., T. Yoshiki, and E. Fleissner.** 1976. A core polyprotein of murine leukemia virus on the surface of mouse leukemia cells. Cell **9**:573–578.
40. **Weiss, R.** 1969. Interference and neutralization studies with Bryan strain Rous sarcoma virus synthesized in the absence of helper virus. J. Gen. Virol. **5**:529–539.
41. **Weiss, R., N. Teich, H. E. Varmus, and J. Coffin (ed.).** 1984. RNA tumor viruses, 2nd ed. Cold Spring Harbor Laboratory, Cold Spring Harbor, N.Y.
42. **Witte, O. N., and D. Baltimore.** 1978. Relationship of retrovirus polyprotein cleavages to virion maturation studied with temperature-sensitive murine leukemia virus mutants. J. Virol. **26**:750–761.